Check for updates

Insight into the dynamic transformation properties of microplastic-derived dissolved organic matter and its contribution to the formation of chlorination disinfection by-products†

Yingyue Zhou,* Feng Zeng, [ID] Kunyan Cui, Longxia Lan, Hao Wang and Weiqian Liang [ID] *

Microplastics (MPs) can cause adverse effects and pose potential threats to humans and the environment. In addition, dissolved organic matter leached from MPs (MP-DOM) is also a critical issue due to its ecotoxicity and potential to form disinfection by-products (DBPs) during the disinfection process of water treatment plants. However, limited information is available on the dynamic transformation of MP-DOM during UV irradiation and subsequent disinfection, which may further influence the formation of DBPs in MP-DOM. Herein, PSMPs-DOM were leached in aqueous solutions under UV irradiation and the samples were then chlorinated. PSMPs-DOM before and after chlorination were characterized by multiple spectral technologies and methods. With prolonged irradiation time, the aromaticity, molecular weight, humic-like substances and oxygen-containing functional groups of PSMPs-DOM increased, suggesting the continuous transformation of PSMPs-DOM. After chlorination, the aromaticity, molecular weight and humic-like substances of PSMPs-DOM decreased, among which the changes of C2 and oxygen-containing functional groups were more significant. Besides, the PSMPs-DOM formed under prolonged irradiation exhibited higher chlorine reactivity, owing to the more aromatic structures and unsaturated bonds. TCM, DCBM, DBCM and TBM were detected in all chlorinated PSMPs-DOM samples, while the PSMPs-DOM formed at the later stage of irradiation exhibited lower THMs formation potential. The correlation results showed that the conversion of humic-like substances in PSMPs-DOM affected the THMs formation potential, with photo-induced humic-like substance being a more dominant factor. This study provided more information on the relationship between the compositional transformation of MP-DOM and their potential to form DBPs, which may facilitate the assessment of potential toxicity associated with MPs-containing water, as well as the development of more effective water treatment methods.

1. Introduction

Microplastics (MPs), typically defined as plastic particles with a size smaller than 5 mm,[1] have drawn increasing concern in recent years due to their widespread presence in soils and aquatic ecosystems globally.[2] These small particles can be ingested or taken up by plants or animals and accumulated in the food web, posing a potential threat to both organisms and humans.[3,4] In addition, MPs can be vectors of heavy metals, organic pollutants and pathogenic microorganisms due to their large specific surface area, increasing their environmental risks.[5,6]

School of Chemistry, Sun Yat-sen University, Guangzhou, 510000, China. E-mail: qian378378@163.com; Zhou-Yingyue@hotmail.com; Tel: +86-020-84114133

† Electronic supplementary information (ESI) available. See DOI: https://doi.org/10.1039/d4ra05857g

MPs are widespread in the environment, particularly in the aquatic environment. It is estimated that between 4.8 and 12.7 million metric tonnes of secondary MPs are introduced into the oceans every year.[7] Various levels of MPs have also been detected in fresh water. For example, in the Jinjiang River Basin, the average concentration of MPs in surface water and groundwater was 1.6 and 2.7 particles per L, respectively.[8] Studies in Italy and Finland found MPs concentrations in lake water ranging from 0.057–8.82 and 0.0037–0.66 particles per L, while lakes in North America contained 0.028–19.1 particles per L MPs.[9] Besides, recent research has also detected MPs in water treatment plants (WTPs), since fresh water such as rivers and lakes are the main sources for WTPs.[10] It is reported that the concentration of MPs in different drinking water plants ranged from less than 2.5 to more than 100 particles per L.[11] In the influent of wastewater treatment plants (WWTPs), the MPs levels varied from 1 to 10 044 particles per L. And the concentrations of MPs in the

effluent of WWTPs were in the range of 0 to 447 particles per L.[12] MPs can remain in the environment for a long period, during which the decomposition of MPs occur *via* physical, chemical and biological paths,[13,14] facilitating the release of microplastic-derived dissolved organic matter (MP-DOM).[15] MP-DOM consists of various chemicals such as additives and copolymers of MPs, which has attracted increasing attention as a potential threat to the environment.[16,17] Ultraviolet irradiation is considered to be an important pathway for the generation of MP-DOM,[18] and several studies have shown the increasing release of MP-DOM under UV conditions. For example, Lee *et al.* found that the dissolved organic carbon concentrations of MP-DOM became almost 100 times greater than those under dark conditions.[16] During UV irradiation, MPs undergo complex physical and chemical transformations, which affect the leaching of MP-DOM,[19] but information on compositional changes of MP-DOM during this process are still limited. Therefore, more detailed research should be carried out to further investigate the leaching characteristics of MP-DOM during UV irradiation.

Moreover, many studies have demonstrated that MP-DOM can react with disinfectants in water treatment processes, resulting in the formation of disinfection by-products (DBPs), which were considered to be carcinogenic, teratogenic, cytotoxic and genotoxic, posing adverse effects on aquatic ecosystems and human health.[20,21] Lee *et al.* first demonstrated that the MP-DOM can act as a trichloromethane (TCM) precursor in chlorination.[16] And it is reported that TCM is the dominant by-products during the chlorination of MP-DOM,[19,22,23] while the species may be converted to more toxic brominated DBPs due to the release of Br⁻ from MPs.[15] In addition, Ateia *et al.* found that the DBPs formation potential of MP-DOM significantly depended on the type of MPs by investigating different kinds of MP-DOM.[24] However, little is known about the changes in the properties of MP-DOM during disinfection and the contribution of components in MP-DOM to the formation of DBPs. Therefore, the transformation of MP-DOM during disinfection and the relationship between the properties of MP-DOM and their DBPs formation potential need to be further explored.

The aim of this study was to investigate the dynamic transformation of MP-DOM during UV irradiation and subsequent disinfection, and the contribution of components in MP-DOM to the formation of DBPs. Polystyrene microplastics (PSMPs) were chosen as typical microplastics due to it is one of the most used plastics and widely distributed in the environment.[25] And chlorine was selected as typical disinfectants since it is most widely used for disinfection in water treatment process.[26] The leaching of PSMPs-DOM was conducted in water solutions under UV light conditions. And the leached PSMPs-DOM were treated by the chlorination. The structure and composition of PSMPs-DOM before and after chlorination were analyzed using UV–vis spectroscopy, excitation–emission matrix (EEM), and Fourier transform infrared (FTIR) combined with parallel factor (PARAFAC) analysis and two-dimensional correlation spectroscopy (2D-COS). And the concentration of THMs was determined by GC-ECD. Meanwhile, the relationship between the properties of MP-DOM and their DBPs formation potential were

investigated by correlation analysis and principal component analysis. The results of this study may provide a deeper insight into the compositional transformation of MP-DOM and its formation potential of chlorination DBPs.

2. Materials and methods

2.1 Materials and chemicals

PSMPs (0.3–0.5 mm) were purchased from Shenghao plastics Co., Ltd (Dongguan, China). THMs mixed standards (tribromomethane (TBM), bromodichloromethane (DCBM), dibromochloromethane (DBCM) and trichloromethane (TCM)) were purchased from Anpel (Shanghai, China). Methyl *tert*-butyl ether (MtBE, HPLC grade) and sodium hypochlorite solution (NaClO, ≥5.0%) were purchased from Aladdin (Shanghai, China). Other chemicals were obtained from Guangzhou Chemical Reagent Co., Ltd (Guangzhou, China). All chemicals in this study were of analytical grade and used without purification unless specifically stated. Ultrapure water (18.2 MΩ) was produced using a Milli-Q system (Millipore, USA).

2.2 The leaching experiments of PSMPs-DOM

PSMPs were rinsed with ultrapure water and dried at 25 °C for 48 h.[27] The clean PSMPs were sealed in glass vitals without exposure to light at 25 °C.

PSMPs-DOM leaching experiments were conducted in a hollow photoreactor equipped with a UVC-254 lamp (TUV 16w T5 4P-SE) under continuous agitation and recirculating cooling system (25.0 ± 0.5 °C). In this experiment, the average UV intensity was determined to be approximately 0.51 mW cm⁻². 10 g PSMPs were mixed with 1000 mL of ultrapure water and placed in a glass beaker. The mixtures were then uniformly dispersed by magnetic stirring. Control experiments were conducted under the same conditions without UV irradiation. The PSMPs suspensions were collected at predetermined reaction intervals (*i.e.*, 6, 12, 30, 54, 84 and 120 h), and filtered by a pre-washed filter with 0.45 μm membrane. The filtrates (PSMPs-DOM$_x$, x was the time of UV irradiation) were stored in refrigerator at 4 °C for further chlorination.

2.3 The chlorination of PSMPs-DOM

The chlorination experiment was conducted in 25 mL glass tubes with stopper on an oscillator in the dark at 25.0 ± 0.5 °C. 20 mL PSMPs-DOM samples were mixed with sodium hypochlorite to achieve 0 (as controls), 10, 50 and 100 mg L⁻¹ available chlorine concentration. The mixing solution pH were kept in the range of 6–7 using hydrochloric acid (HCl) or sodium hydroxide (NaOH). The samples were withdrawn after 24 h and quenched with ascorbic acid.[22] An aliquot of the quenched samples was extracted for analysis of THMs, and the others were used to investigate the properties of chlorinated PSMPs-DOM. The control groups were also performed following the above procedure without the addition of sodium hypochlorite solution.

2.4 Analytical methods

Dissolved organic matter (DOC) was measured using a DOC-VCSH analyzer (Shimadzu, Japan). The UV-vis absorption spectra of the PSMPs-DOM solutions were collected using a UV-vis spectrophotometer (Lambda 950, PerkinElmer). The absorption coefficient at 254 nm (α_{254}) was used to indicate the extent of DOM aromaticity.[28] The spectral slope (S, nm^{-1}) was obtained by a non-linear exponential decay model, and $S_{275-295}$ was the S value at wavelengths of 275–295 nm. This value was used to characterize the relative molecular size of the DOM.[28] Fourier transform infrared (ATR-FTIR) spectra of PSMPs and PSMPs-DOM were recorded on a FTIR spectrometer (Thermo Scientific, USA). The excitation emission matrix (EEM) and synchronous fluorescence spectra of the PSMPs-DOM were measured using a fluorophotometer (RF-5301 PC, Shimadzu, Japan). The surface morphology of PSMPs was characterized by a scanning electron microscope (SU8010, Hitachi, Japan). The concentration of THMs were quantified by gas chromatography (Agilent Technologies 7820A, USA), equipped with electron capture detector (ECD) and HP-5 column (30 m × 0.32 mm × 0.25 μm) based on USEPA 551.1.[22] pH was measured by pH-meter (FiveEasy Plus, Mettler Toledo). All samples were subjected to three parallel experiments. Detailed information was summarized in ESI.†

2.5 Statistical analysis

2D-COS analysis for the spectral data was performed using the 2D Shige software (2D-Shige version 1.3, https://sites.google.com/site/Shigemorita/home/2dshige). The DOMFlour and drEEM toolboxes were used for the PARAFAC of fluorescence spectral data. The graphs were plotted with Origin Pro 9.0. More detailed information about data analysis was described in ESI.†

3. Results and discussion

3.1 The leaching characteristics of PSMPs-DOM under UV irradiation

As shown in Fig. 1 and S1,† the morphology and functional groups of the pristine and UV-irradiated PSMPs showed distinct changes, which were consistent with previous studies.[29,30] Compared to the untreated PSMPs, the cracks, flakes and debris on the surface of the UV-irradiated PSMPs became significant, and the peak intensities at 3746 cm^{-1}, 1730 cm^{-1} and 1066 cm^{-1} of the PSMPs increased after UV irradiation, corresponding to –OH, C=O and C–O, respectively.[27] Meanwhile, the intensity of the peaks at 2973 cm^{-1} and 2902 cm^{-1}, which are associated with asymmetric stretching vibrations of –CH as well as –CH$_2$, decreased after UV irradiation, suggesting the damage to backbone of PSMPs.[19,31] The changes of structures and properties in PSMPs may further affect the release of PSMPs-DOM.[32]

The DOC concentration showed a gradual upward trend, increasing rapidly during the first 54 h and then slowing down,
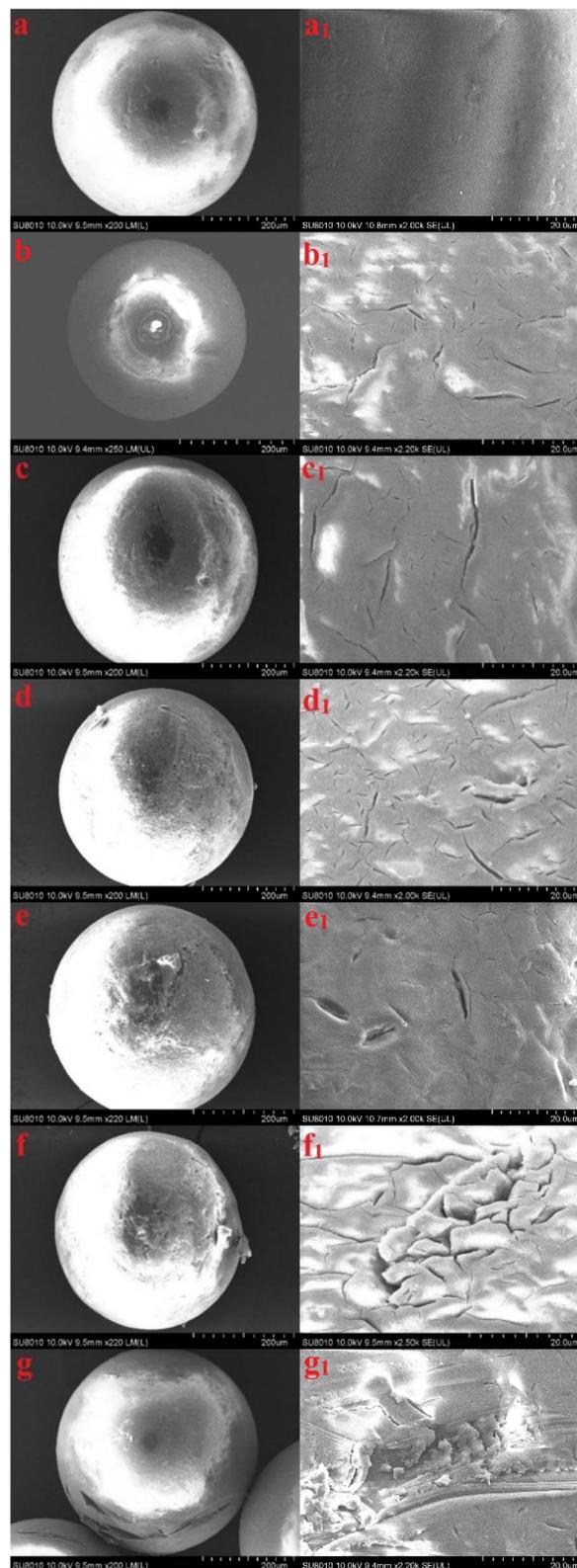

Fig. 1 SEM micrographs of original PSMPs (a and a$_1$) and irradiated PSMPs under 6, 12, 30, 54, 84, and 120 h UV irradiation (b and b$_1$–g and g$_1$).

from 8.71 mg C per L to 214 mg C per L (Table S4†), since the cracking and fragmentation of PSMPs under UV irradiation promoted the release of PSMPs-DOM,[27,33] while the rough surface can also facilitate the adsorption of PSMPs-DOM onto MPs.[31] In addition, the released PSMPs-DOM may further undergo photodegradation process.[30,34]

Fig. S2† showed that the UV absorption peak appeared in the range of 200–260 nm, which were related to the C=C, C=O, and benzene ring structures.[19,35] During UV irradiation for 6–84 h, the absorbance was gradually enhanced and the wavelength was red-shifted with the increasing irradiation time, which was due to the formation and expansion of conjugated system in PSMPs-DOM.[36] However, the absorbance decreased as

for the PSMPs-DOM formed under 120 h UV irradiation. PSMPs-DOM contained chromophores such as C=O and C=C with significant photoreactive activity, resulting in photodegradation of PSMPs-DOM under continuous UV irradiation.[34] As shown in Table S5,† α_{254} increased first and then decreased, indicating that UV irradiation promoted the release of aromatic substances from PSMPs, but it may also lead to the photo-degradation of PSMPs-DOM, destroying the aromatic structure.[34]

As seen in Fig. S3,† PSMPs-DOM† had a strong and broad fluorescence peak (Ex/Em = 300–350 nm/400–460 nm), which can be inferred as the humic-like substances.[29] With increasing irradiation time, the peak intensity first increased but then
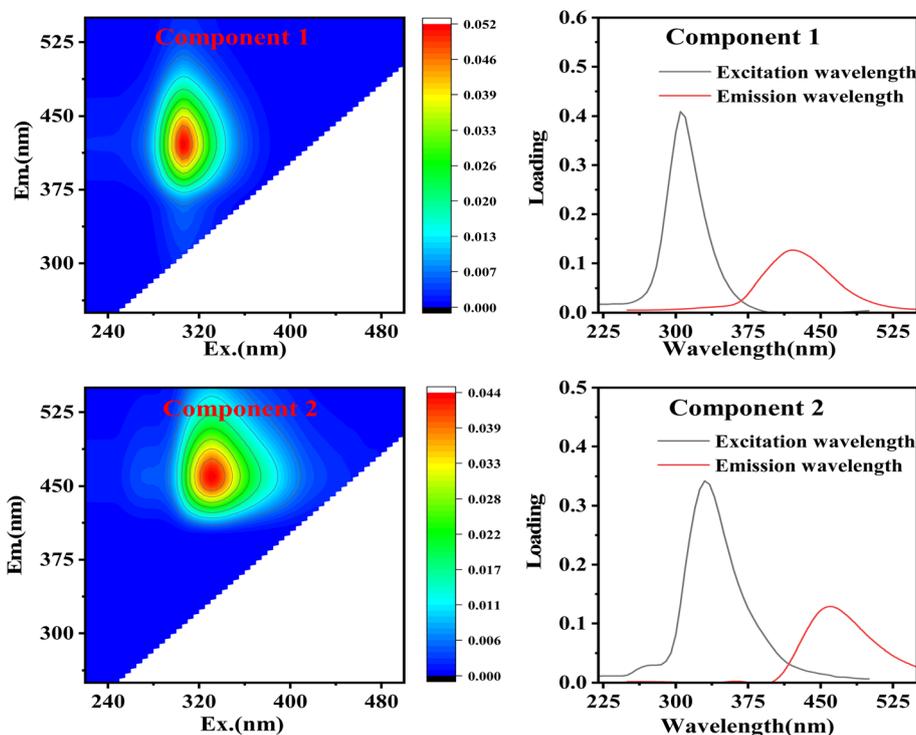

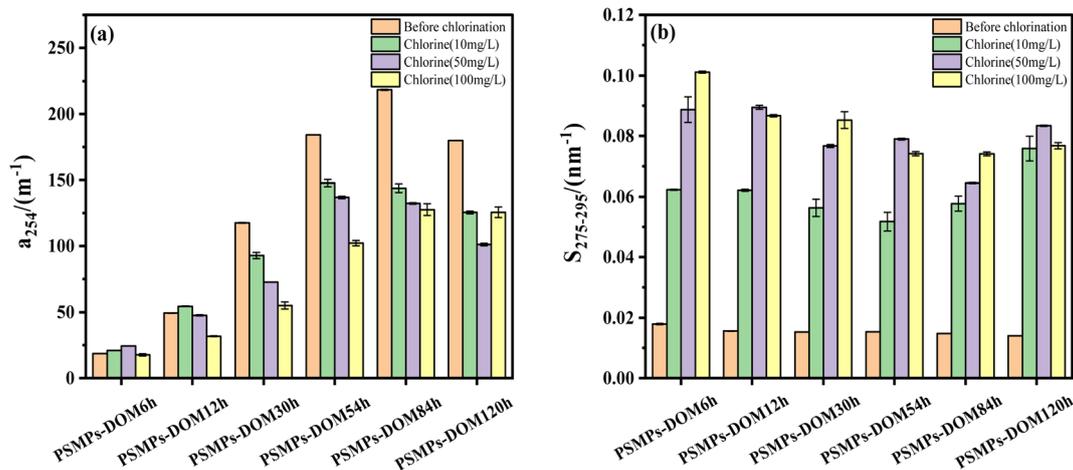**Fig. 2** EEM-PARAFAC components of PSMPs-DOM.

Fig. 3 α_{254} (a) and $S_{275-295}$ (b) of PSMPs-DOM before and after chlorination.

decreased slightly, revealing that UV irradiation promoted the release of fluorescent substances in PSMPs, while continuous irradiation resulted in the photodegradation of humic-like components.[31] And the fluorescent wavelength of PSMPs-DOM was red-shifted with increasing UV irradiation time (Fig. S4†), which was attributed to the increasing content of aromatic moieties and oxygen-containing functional groups such as carbonyl, hydroxyl, carboxyl and alkoxy groups.[37] Two components were obtained by EEM-PARAFAC (Fig. 2), where C1 was photo-induced humic-like substance while C2 was the component similar to terrestrial humic-like substances with higher molecular weight.[38,39] And the longer excitation and emission wavelengths of C2 may be related to its more complex conjugated aromatic structure.[40] As shown in Table S6,† during the leaching process, $F_{max}(C1)$ and $F_{max}(C2)$ increased from 438 and 119 to 1866 and 1433 respectively, indicating that the leached PSMPs-DOM contained more C1. In addition, the fluorescence intensity of C2 decreased while that of C1 continued to increase at the late stage of irradiation, probably due to the photodegradation of C2 and part of C2 may be converted to C1.[30]

The changes of functional groups in PSMPs-DOM during UV irradiation were analyzed by FTIR spectrophotometry (Fig. S5†). The peak at around 2900 cm^{-1} corresponded to the stretching vibration of the C–H bond, with enhancement reflecting the increase of aliphatic substances in PSMPs-DOM.[35] The peak at 1720 cm^{-1} and 1200 cm^{-1} were related to the C=O and C–O respectively, increasing with the prolonged UV irradiation.[35,41] The absorption peak at 1600–1650 cm^{-1} represented the aromatic C=C bond, of which intensity decreased at the late stage of UV irradiation, revealing part of aromatic structures were destroyed.[39] The increase of oxygen-containing functional groups was consistent with the changes in the UV and fluorescence spectra of PSMPs-DOM, as the increase in humic-like substances was associated with the appearance of carbonyl, hydroxyl and carboxyl groups. Nevertheless, with increasing irradiation time, some of the aromatic structures of PSMPs-DOM were photodegraded and converted to substances containing saturated aliphatic chains.

3.2 The dynamic transformation of PSMPs-DOM during chlorination

As shown in Fig. S6,† the DOC concentration decreased by 11.86 mg C per L at 10 mg L^{-1} chlorination, while the values decreased by 60.85 and 57.87 mg C per L at higher chlorination concentrations (50 and 100 mg L^{-1}), as some of the PSMPs-DOM was probably oxidized to CO$_2$ during the chlorination,[42] and more available chlorine in the solution can further promote the oxidization. Similarly, the UV absorbance of chlorinated PSMPs-DOM almost all decreased to different degrees, suggesting the reaction of UV-absorbing substances in PSMPs-DOM during chlorination (Fig. S7†).

It is showed that the chlorinated PSMPs-DOM exhibited an absorption peak at 250–270 nm with a relatively small absorbance attenuation, which may be attributed to the chlorination products (*i.e.*, quinones and aromatic ketones) as well as the chlorine-resistant chromophores.[42,43] Comparatively, the

absorbance decreased more obviously in the range of 300–400 nm, since the absorption at long wavelengths were attributed to the larger conjugated structures in PSMPs-DOM, which exhibited relatively high chlorine reactivity.[42] Moreover, these substances may transform into the ones with low absorption at long wavelengths.[44]

The α_{254} of PSMPs-DOM decreased and $S_{275-295}$ increased after chlorination (Fig. 3), suggesting the reduction of aromaticity and molecular weight of PSMPs-DOM. Aromatic structures
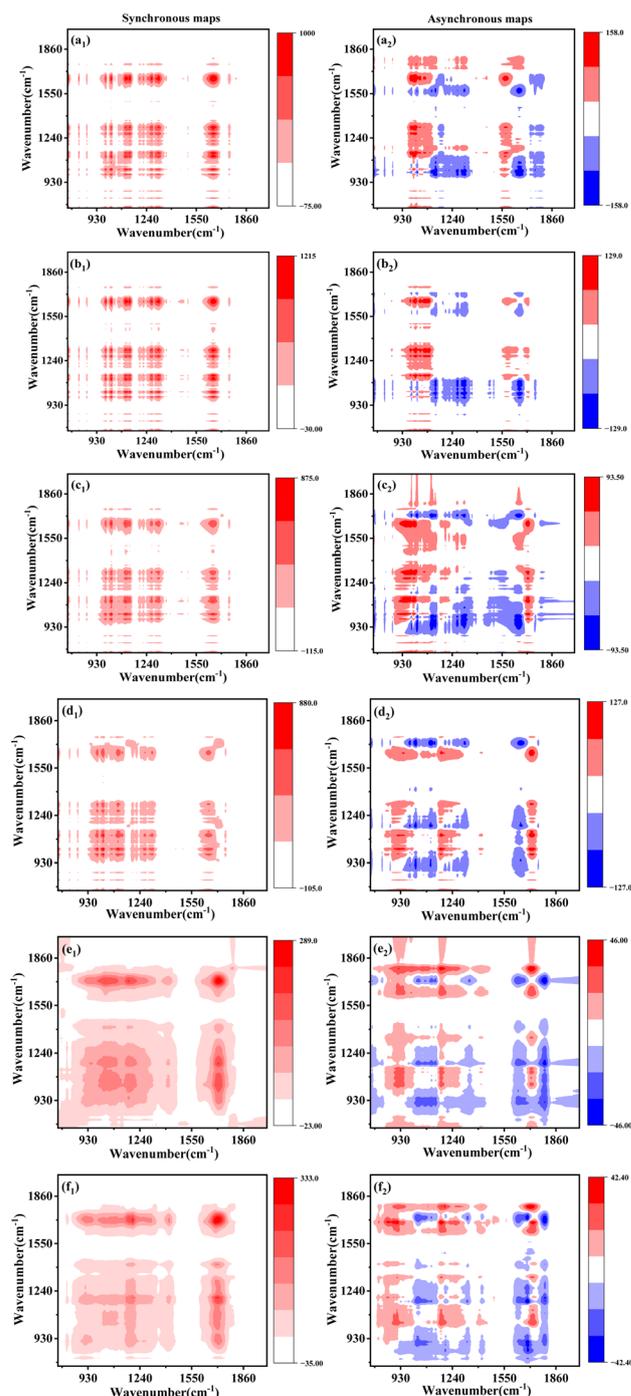

Fig. 4 2D-FTIR-COS spectra of PSMPs-DOM$_x$ after chlorination ((a$_1$), (a$_2$)–(f$_1$), (f$_2$), x = 6, 12, 30, 54, 84, 120 h).

and unsaturated bonds of PSMPs-DOM were prone to react with chlorine, resulting in the formation of aliphatic compounds or small molecules products.[45] As shown in Table S7,† the changes in the aromaticity of PSMPs-DOM formed under longer UV irradiation time were more obvious and drastic, indicating that these PSMPs-DOM contained more structures or substances with higher chlorine reactivity. With increasing dosage of chlorine, the α_{254} and $S_{275-295}$ changed more significantly as well, since the reactive species involved in the reaction (*e.g.*, chlorine radicals and hydroxyl radicals) change with the concentration of chlorine, which in turn affected the rate and extent of the reaction.

In Fig. S11,† the fluorescence intensity of humic-like substances decreased after chlorination, indicating that some of the fluorescent substances were degraded, and the increasing chlorine dosage will facilitate the reaction, which was consistent with the previous study.[46] The changes of F_{max} values were similar to those of UV parameters (Fig. S12†), which further demonstrated that PSMPs-DOM formed at the later stage of UV irradiation contained structures and substances with higher

chlorine reactivity. As illustrated in Table S8,† it can be found that C1 and C2 showed different trend during chlorination. For the PSMPs-DOM formed under the identical irradiation time, the relative content of C1 almost increased while that of C2 decreased after chlorination, which was probably due to that part of C2 converted into C1 with relatively small molecular weight during chlorination.[47]

To get more insights of critical groups transformation in PSMPs-DOM during chlorination, 2D-COS analysis of the FTIR spectra (Fig. S13 and Table S9†) was conducted. As shown in Fig. 4, five auto-peaks at 1654, 1314, 1270, 1139, 1022 cm^{-1} and a small peak at 1721 cm^{-1} occurred in the synchronous maps of the PSMPs-DOM formed at the initial 54 h, whereas only one predominant auto-peak centered at 1721 cm^{-1}, and small peaks at 1139 and 1022 cm^{-1} presented in the synchronous maps of the PSMPs-DOM formed under 84 and 120 h UV irradiation. According to previous studies, the peaks appeared at 1721, 1654, 1314, 1270, 1139 and 1022 cm^{-1} were attributed to the O–C=O, aromatic C=C/C=O, C–OH, C–O, C–O–C and aromatic C–H respectively.[48,49] The positive cross-peaks were detected in
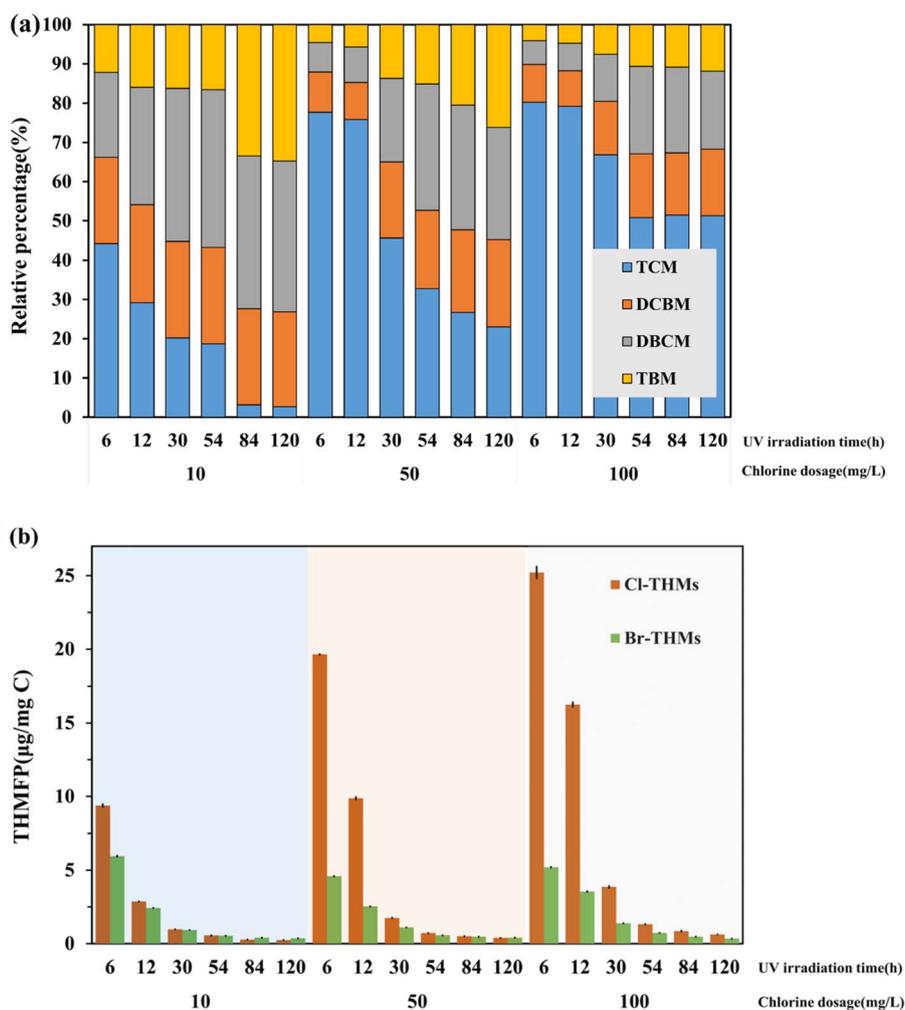

Fig. 5 (a) The relative percentage of each THMs produced from PSMPs-DOM during chlorination (b) formation potential of Cl-THMs and Br-THMs in PSMPs-DOM during chlorination.

all synchronous maps, indicating that these functional groups changed simultaneously during chlorination. Contrarily, the cross-peak signals in the asynchronous maps showed significant differences and specific signatures of the cross-peaks recognized from the asynchronous maps were listed in Table S10.† Based on Noda's rules, it can be found that the oxygen-containing functional groups (*e.g.*, C=O and C–O–C) in PSMPs-DOM show the fastest transformation during chlorination, which was consistent with the conclusion that oxygen-containing functional groups have higher chlorine reactivity.[50]

3.3 Influence of PSMPs-DOM properties to the formation potential of chlorination DBPs

Four THMs, including TCM, DCBM, DBCM and TBM were detected in all chlorinated PSMPs-DOM samples. As shown in Table S11,† with chlorine dosage raised from 10 to 100 mg L^{-1}, the formation potential of THMs increased distinctly, especially in the PSMPs-DOM samples formed under 6 h UV irradiation. The formation potential ranged from 0.01 to 21.1 µg per mg C for TCM, 0.09 to 2.52 µg per mg C for DCBM, 0.14 to 2.31 µg per mg C for DBCM, and 0.08 to 1.30 µg per mg C for TBM respectively. The relative concentration of THMs in each PSMPs-DOM after chlorination were shown in Fig. 5(a). It is evident that TCM was abundant in PSMPs-DOM samples, ranging from

2.67% to 80.2%, followed by DCBM and DBCM, ranging from 8.99% to 24.9% and from 6.05% to 40.2%. Besides, with increasing chlorine dosage, the formation potential of brominated species (*e.g.*, TBM and DBCM) showed decreasing and opposite trends to that of the Cl-THMs (*e.g.*, TCM and DCBM) (Fig. 5(b)), which was probably due to the transformation and decomposition of different THMs species.[51,52]

In the Fig. 6, $S_{275-295}$ was positively correlated with the total THMs formation potential, suggesting that PSMPs-DOM with lower molecular weight was more likely to form THMs during chlorination, which complied with the conclusion that DOM with relatively small molecular weight are the main precursors of THMs.[16] Differently, the α_{254} of PSMPs-DOM showed negative correlation with the total THMs formation potential, indicating that not all substances with aromatic structures react with chlorine to produce THMs, and some compounds contributing to the UV absorbance of PSMPs-DOM may be inert with respect to THMs formation.[53] According to the above analysis, it was known that PSMPs-DOM contained more humic-like fluorescent components with increasing irradiation time, reflecting that the structure of PSMPs-DOM became more compact and complex, making it more likely that PSMPs-DOM would first be degraded into small molecules products rather than directly oxidized to produce THMs.
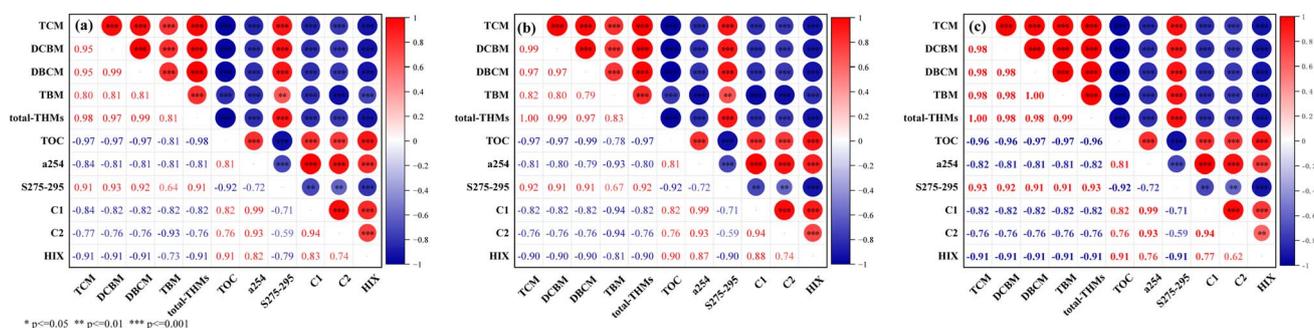

Fig. 6 Spearman correlation analysis between properties of PSMPs-DOM and its THMFP ((a)–(c), 10, 50, 100 mg L^{-1} chlorine dosage).
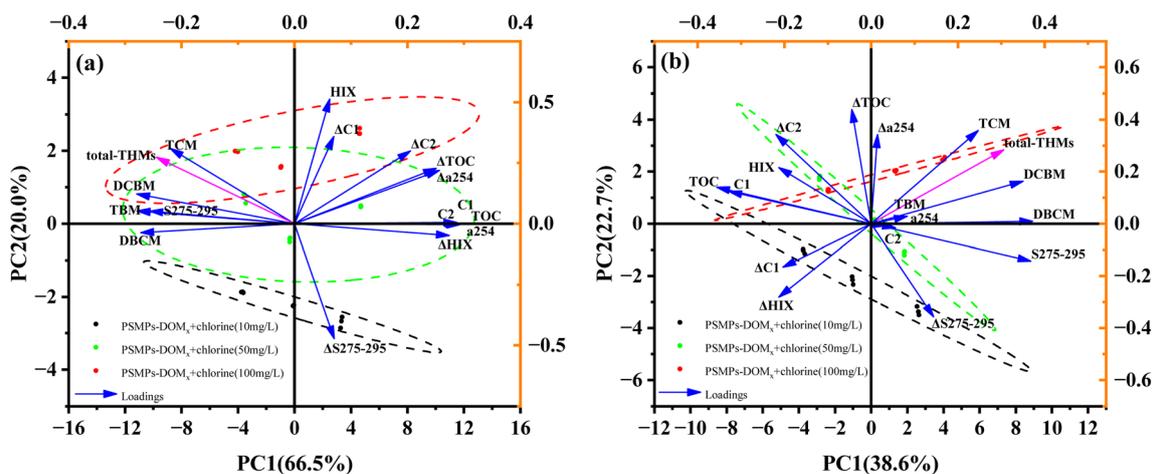

Fig. 7 (a) Principal component analysis between properties of PSMPs-DOM$_x$ (x = 6, 12, 30 h) and its THMFP; (b) principal component analysis between properties of PSMPs-DOM$_x$ (x = 54, 84, 120 h) and its THMFP.

To obtain further insight into the relative contributions of PSMPs-DOM properties to the formation of THMs during chlorination, principal component analysis was performed, which explained the total variance of 66.5% and 20.0%, 38.6% and 22.7% for the PC1 and PC2 in the initial 30 h and prolonged UV irradiation (Fig. 7). Similar to the correlation plot, it is showed that $\Delta\alpha_{254}$, ΔHIX and $\Delta S_{275-295}$ can represent the complete compositional variation of the PSMPs-DOM during chlorination. The formation potential of total THMs were inversely distributed with C1 and C2 along the PC1 axis in PSMPs-DOM samples formed during 6 to 30 h UV irradiation. However, as for the PSMPs-DOM produced under 54 to 120 h UV irradiation, the formation potential of total THMs and C2 were in the positive direction of the PC1 axis, while C1 was distributed in the negative axis of PC1, indicating the change of humic-like substances in PSMPs-DOM affected the formation of THMs during chlorination. With increasing irradiation time, the correlation between ΔC1 and the formation potential of total THMs along the PC2 axis became negative, and the contribution of ΔC1 to the formation potential of total THMs decreased, suggesting that compared to C2, the photo-induced humic-like component (C1) may be a more dominant factor influencing the formation potential of THMs in PSMPs-DOM. Meanwhile, the contribution of C1 to the formation of THMs in the PSMPs-DOM formed under prolonged irradiation was not as significant as that in the early stage of UV irradiation.

4. Conclusions

In this study, the compositional changes of PSMPs-DOM during UV irradiation and subsequent chlorination, and the correlation between the properties of PSMPs-DOM and their potential to form THMs were investigated. The main conclusions according to the results were as followed:

(1) The surface properties of PSMPs changed substantially during UV irradiation, which influenced the release of PSMPs-DOM. With increasing irradiation time, the aromaticity, molecular weight, humic-like substances and oxygen-containing functional groups of PSMPs-DOM increased, suggesting the continuous transformation of PSMPs-DOM.

(2) After chlorination, the aromaticity, molecular weight and humic-like substances of PSMPs-DOM decreased, among which the changes of C2 and oxygen-containing functional groups were more significant. Besides, the PSMPs-DOM formed under prolonged irradiation exhibited higher chlorine reactivity, which was probably due to the more aromatic structures and unsaturated bonds.

(3) TCM, DCBM, DBCM and TBM were detected in all chlorinated PSMPs-DOM samples, and opposite trends were observed between chlorinated and brominated THMs formation potential. However, in contrast to the chlorine reactivity, the PSMPs-DOM formed under prolonged irradiation exhibited lower potential to THMs formation, indicating that PSMPs-DOM with higher aromaticity and more complex structures may not be the main precursors of THMs. The correlation results showed that the conversion of humic-like substances in PSMPs-DOM influenced the THMs formation potential, with C1

being a more dominant factor compared to C2. Moreover, the contribution of C1 to the formation of THMs in the PSMPs-DOM formed under prolonged irradiation was not as significant as that in the early stage of UV irradiation.

The results of this study showed that the formation and components of DBPs differed when MPs-containing water experienced varying periods of UV irradiation, emphasizing the need for corresponding assessment of different sources of water that may contain substantial MPs before the disinfection process, which were significant for both water security and the aquatic environment.

Consent to participate

All authors have given consent to their contribution.

Consent for publication

All authors have agreed with the content and all have given explicit consent to publish.

Data availability

The data supporting this article have been included as part of the ESI.†

Author contributions

Yingyue Zhou: conceptualization, methodology, validation, formal analysis, investigation, data curation, writing-original draft, visualization; Feng Zeng: supervision, writing-original draft, writing-review & editing; Kunyan Cui: validation, formal analysis, investigation, data curation; Longxia Lan: data curation, writing-Review & editing; Hao Wang: formal analysis, methodology, investigation; Weiqian Liang: conceptualization, methodology, writing-original draft, writing-review & editing.

Conflicts of interest

There are no conflicts to declare.

Acknowledgements

References

1 Y. Deng, J. Wu, J. Chen and K. Kang, Overview of microplastic pollution and its influence on the health of organisms, *J. Environ. Sci. Health, Part A: Toxic/Hazard. Subst. Environ. Eng.*, 2023, **58**, 412–422.

2 N. Kasmuri, N. A. A. Tarmizi and A. Mojiri, Occurrence, impact, toxicity, and degradation methods of microplastics in environment—a review, *Environ. Sci. Pollut. Res.*, 2022, **29**, 30820–30836.

3 L. Lu, T. Luo, Y. Zhao, C. Cai, Z. Fu and Y. Jin, Interaction between microplastics and microorganism as well as gut microbiota: A consideration on environmental animal and human health, *Sci. Total Environ.*, 2019, **667**, 94–100.

4 M. Kumar, X. Xiong, M. He, D. C. W. Tsang, J. Gupta, E. Khan, S. Harrad, D. Hou, Y. S. Ok and N. S. Bolan, Microplastics as pollutants in agricultural soils, *Environ. Pollut.*, 2020, **265**, 114980.

5 A. Ter Halle, L. Ladirat, X. Gendre, D. Goudouneche, C. Pusineri, C. Routaboul, C. Tenailleau, B. Duployer and E. Perez, Understanding the fragmentation pattern of marine plastic debris, *Environ. Sci. Technol.*, 2016, **50**, 5668–5675.

6 A. W. Verla, C. E. Enyoh, E. N. Verla and K. O. Nwarnorh, Microplastic–toxic chemical interaction: a review study on quantified levels, mechanism and implication, *SN Appl. Sci.*, 2019, **1**, 1400.

7 J. Boucher and D. Friot, *Primary Microplastics in the Oceans: A Global Evaluation of Sources*, IUCN International Union for Conservation of Nature, 2017.

8 Y. Liu, L. Wu, G. Shi, S. Cao and Y. Li, Characteristics and sources of microplastic pollution in the water and sediments of the Jinjiang River Basin, *China Geology*, 2022, **5**, 1–10.

9 S. Yang, M. Zhou, X. Chen, L. Hu, Y. Xu, W. Fu and C. Li, A comparative review of microplastics in lake systems from different countries and regions, *Chemosphere*, 2022, **286**, 131806.

10 K. Nirmala, G. Rangasamy, M. Ramya, V. U. Shankar and G. Rajesh, A critical review on recent research progress on microplastic pollutants in drinking water, *Environ. Res.*, 2023, **222**, 115312.

11 L. Yang, S. Kang, X. Luo and Z. Wang, Microplastics in drinking water: A review on methods, occurrence, sources, and potential risks assessment, *Environ. Pollut.*, 2024, **348**, 123857.

12 J. Sun, X. Dai, Q. Wang, M. C. M. Van Loosdrecht and B.-J. Ni, Microplastics in wastewater treatment plants: Detection, occurrence and removal, *Water Res.*, 2019, **152**, 21–37.

13 O. S. Alimi, D. Claveau-Mallet, R. S. Kurusu, M. Lapointe, S. Bayen and N. Tufenkji, Weathering pathways and protocols for environmentally relevant microplastics and nanoplastics: What are we missing?, *J. Hazard. Mater.*, 2022, **423**, 126955.

14 B. Gewert, M. M. Plassmann and M. MacLeod, Pathways for degradation of plastic polymers floating in the marine environment, *Environ. Sci.: Processes Impacts*, 2015, **17**, 1513–1521.

15 Y. K. Lee, H.-Y. Yoo, K.-S. Ko, W. He, T. Karanfil and J. Hur, Tracing microplastic (MP)-derived dissolved organic matter in the infiltration of MP-contaminated sand system and its disinfection byproducts formation, *Water Res.*, 2022, **221**, 118806.

16 Y. K. Lee, C. Romera-Castillo, S. Hong and J. Hur, Characteristics of microplastic polymer-derived dissolved organic matter and its potential as a disinfection byproduct precursor, *Water Res.*, 2020, **175**, 115678.

17 T. J. Suhrhoff and B. M. Scholz-Böttcher, Qualitative impact of salinity, UV radiation and turbulence on leaching of organic plastic additives from four common plastics — A lab experiment, *Mar. Pollut. Bull.*, 2016, **102**, 84–94.

18 A. Potthoff, K. Oelschlägel, M. Schmitt-Jansen, C. D. Rummel and D. Kühnel, From the sea to the laboratory: Characterization of microplastic as prerequisite for the assessment of ecotoxicological impact, *Integr. Environ. Assess. Manage.*, 2017, **13**, 500–504.

19 L. Zhou, R. Ma, C. Yan, J. Wu, Y. Zhang, J. Zhou, G. Qu, X. He and T. Wang, Plasma-mediated aging process of different microplastics: Release of dissolved organic matter and formation of disinfection by-products, *Sep. Purif. Technol.*, 2022, **303**, 122143.

20 S. Kali, M. Khan, M. S. Ghaffar, S. Rasheed, A. Waseem, M. M. Iqbal, M. Bilal Khan Niazi and M. I. Zafar, Occurrence, influencing factors, toxicity, regulations, and abatement approaches for disinfection by-products in chlorinated drinking water: A comprehensive review, *Environ. Pollut.*, 2021, **281**, 116950.

21 E. D. Wagner and M. J. Plewa, CHO cell cytotoxicity and genotoxicity analyses of disinfection by-products: An updated review, *J. Environ. Sci.*, 2017, **58**, 64–76.

22 K. Y. Koh, Z. Chen, S. Lin, K. Chandra Mohan, X. Luo and J. P. Chen, Leaching of organic matters and formation of disinfection by-product as a result of presence of microplastics in natural freshwaters, *Chemosphere*, 2022, **299**, 134300.

23 Z. Yan, H. Qian, J. Yao, M. Guo, X. Zhao, N. Gao and Z. Zhang, Mechanistic insight into the role of typical microplastics in chlorination disinfection: Precursors and adsorbents of both MP-DOM and DBPs, *J. Hazard. Mater.*, 2024, **462**, 132716.

24 M. Ateia, A. Kanan and T. Karanfil, Microplastics release precursors of chlorinated and brominated disinfection byproducts in water, *Chemosphere*, 2020, **251**, 126452.

25 X. Lv, Q. Dong, Z. Zuo, Y. Liu, X. Huang and W.-M. Wu, Microplastics in a municipal wastewater treatment plant: Fate, dynamic distribution, removal efficiencies, and control strategies, *J. Cleaner Prod.*, 2019, **225**, 579–586.

26 Y. Li, X. Zhang, M. Yang, J. Liu, W. Li, N. J. D. Graham, X. Li and B. Yang, Three-step effluent chlorination increases disinfection efficiency and reduces DBP formation and toxicity, *Chemosphere*, 2017, **168**, 1302–1308.

27 H. Wang, J. Zhu, Y. He, J. Wang, N. Zeng and X. Zhan, Photoaging process and mechanism of four commonly commercial microplastics, *J. Hazard. Mater.*, 2023, **451**, 131151.

28 J. R. Helms, A. Stubbins, J. D. Ritchie, E. C. Minor, D. J. Kieber and K. Mopper, Absorption spectral slopes and slope ratios as indicators of molecular weight, source, and photobleaching of chromophoric dissolved organic matter, *Limnol. Oceanogr.*, 2008, **53**, 955–969.

29 Y. K. Lee, W. He, H. Guo, T. Karanfil and J. Hur, Effects of organic additives on spectroscopic and molecular-level features of photo-induced dissolved organic matter from microplastics, *Water Res.*, 2023, **242**, 120272.

30 X. Ren, Y. Han, H. Zhao, Z. Zhang, T.-H. Tsui and Q. Wang, Elucidating the characteristic of leachates released from microplastics under different aging conditions: Perspectives of dissolved organic carbon fingerprints and nano-plastics, *Water Res.*, 2023, **233**, 119786.

31 Q. Wang, M. Chen, Y. Min and P. Shi, Aging of polystyrene microplastics by UV/Sodium percarbonate oxidation: Organic release, mechanism, and disinfection by-product formation, *J. Hazard. Mater.*, 2024, **464**, 132934.

32 Z. Ouyang, S. Li, J. Xue, J. Liao, C. Xiao, H. Zhang, X. Li, P. Liu, S. Hu, X. Guo and L. Zhu, Dissolved organic matter derived from biodegradable microplastic promotes photo-aging of coexisting microplastics and alters microbial metabolism, *J. Hazard. Mater.*, 2023, **445**, 130564.

33 Y. K. Lee, K. R. Murphy and J. Hur, Fluorescence signatures of dissolved organic matter leached from microplastics: Polymers and additives, *Environ. Sci. Technol.*, 2020, **54**, 11905–11914.

34 Y. Xu, D. Huang, P. Liu, Z. Ouyang, H. Jia and X. Guo, The characteristics of dissolved organic matter release from UV-aged microplastics and its cytotoxicity on human colonic adenocarcinoma cells, *Sci. Total Environ.*, 2022, **826**, 154177.

35 H. Zhang, W. Qian, L. Wu, S. Yu, R. Wei, W. Chen and J. Ni, Spectral characteristics of dissolved organic carbon (DOC) derived from biomass pyrolysis: Biochar-derived DOC versus smoke-derived DOC, and their differences from natural DOC, *Chemosphere*, 2022, **302**, 134869.

36 S. Dong, X. Yan, Y. Yue, W. Li, W. Luo, Y. Wang, J. Sun, Y. Li, M. Liu and M. Fan, H2O2 concentration influenced the photoaging mechanism and kinetics of polystyrene microplastic under UV irradiation: Direct and indirect photolysis, *J. Cleaner Prod.*, 2022, **380**, 135046.

37 T. Liu, Z. Chen, W. Yu and S. You, Characterization of organic membrane foulants in a submerged membrane bioreactor with pre-ozonation using three-dimensional excitation–emission matrix fluorescence spectroscopy, *Water Res.*, 2011, **45**, 2111–2121.

38 Y. K. Lee, S. Hong and J. Hur, A fluorescence indicator for source discrimination between microplastic-derived dissolved organic matter and aquatic natural organic matter, *Water Res.*, 2021, **207**, 117833.

39 Y. K. Lee, S. Hong and J. Hur, Copper-binding properties of microplastic-derived dissolved organic matter revealed by fluorescence spectroscopy and two-dimensional correlation spectroscopy, *Water Res.*, 2021, **190**, 116775.

40 M. Priyanka and M. P. Saravanakumar, New insights on aging mechanism of microplastics using PARAFAC analysis: Impact on 4-nitrophenol removal via Statistical Physics Interpretation, *Sci. Total Environ.*, 2022, **807**, 150819.

41 C. He, X. He, J. Li, Y. Luo, J. Li, Y. Pei and J. Jiang, The spectral characteristics of biochar-derived dissolved organic matter at different pyrolysis temperatures, *J. Environ. Chem. Eng.*, 2021, **9**, 106075.

42 D. Wan, H. Wang, V. K. Sharma, S. Selvinsimpson, H. Dai, F. Luo, C. Wang and Y. Chen, Mechanistic investigation of enhanced photoreactivity of dissolved organic matter after chlorination, *Environ. Sci. Technol.*, 2021, **55**, 8937–8946.

43 X. Ruan, Y. Xiang, C. Shang, S. Cheng, J. Liu, Z. Hao and X. Yang, Molecular characterization of transformation and halogenation of natural organic matter during the UV/chlorine AOP using FT-ICR mass spectrometry, *J. Environ. Sci.*, 2021, **102**, 24–36.

44 J. Jiang, J. Han and X. Zhang, Nonhalogenated aromatic DBPs in drinking water chlorination: A gap between NOM and halogenated aromatic DBPs, *Environ. Sci. Technol.*, 2020, **54**, 1646–1656.

45 J. Wenk, M. Aeschbacher, E. Salhi, S. Canonica and M. Sander, Chemical oxidation of dissolved organic matter by chlorine dioxide, chlorine, and ozone: Effects on its optical and antioxidant properties, *Environ. Sci. Technol.*, 2013, **47**, 11147–11156.

46 H. V.-M. Nguyen, H.-S. Lee, S.-Y. Lee, J. Hur and H.-S. Shin, Changes in structural characteristics of humic and fulvic acids under chlorination and their association with trihalomethanes and haloacetic acids formation, *Sci. Total Environ.*, 2021, **790**, 148142.

47 Z. Zhou, X. He, M. Zhou and F. Meng, Chemically induced alterations in the characteristics of fouling-causing bio-macromolecules – Implications for the chemical cleaning of fouled membranes, *Water Res.*, 2017, **108**, 115–123.

48 X. Gu, B. Chen, H. Liu, Y. Feng, B. Wang, S. He, M. Feng, G. Pan and S. Han, Photochemical behavior of dissolved organic matter derived from Alternanthera philoxeroides hydrochar: Insights from molecular transformation and photochemically reactive intermediates, *J. Hazard. Mater.*, 2024, **461**, 132591.

49 S. Liu, W. Feng, F. Song, T. Li, W. Guo, B. Wang, H. Wang and F. Wu, Photodegradation of algae and macrophyte-derived dissolved organic matter: A multi-method assessment of DOM transformation, *Limnologica*, 2019, **77**, 125683.

50 X. Wang, H. Zhang, Y. Zhang, Q. Shi, J. Wang, J. Yu and M. Yang, New insights into trihalomethane and haloacetic acid formation potentials: Correlation with the molecular composition of natural organic matter in source water, *Environ. Sci. Technol.*, 2017, **51**, 2015–2021.

51 Z. Hua, D. Li, Z. Wu, D. Wang, Y. Cui, X. Huang, J. Fang and T. An, DBP formation and toxicity alteration during UV/chlorine treatment of wastewater and the effects of ammonia and bromide, *Water Res.*, 2021, **188**, 116549.

52 R. Sinha, A. K. Gupta and P. S. Ghosal, A review on Trihalomethanes and Haloacetic acids in drinking water: Global status, health impact, insights of control and removal technologies, *J. Environ. Chem. Eng.*, 2021, **9**, 106511.

53 J. L. Weishaar, G. R. Aiken, B. A. Bergamaschi, M. S. Fram, R. Fujii and K. Mopper, Evaluation of specific ultraviolet absorbance as an indicator of the chemical composition and reactivity of dissolved organic carbon, *Environ. Sci. Technol.*, 2003, **37**, 4702–4708.